Core Alignment of Butt Coupling Between Single-Mode and Multimode Optical Fibers by Monitoring Brillouin Scattering Signal

Yosuke Mizuno and Kentaro Nakamura, *Member, IEEE*

***Abstract*—We propose a new method to optimize the core alignment of the butt coupling between a single-mode optical fiber (SMF) and a graded-index multimode optical fiber (GI-MMF) by monitoring the spectrum of Brillouin scattered light. This method is stable, free from costly or elaborate equipments, applicable to the coupling of optical fibers with different core diameters or materials, and available even when the power of transmitted light cannot be measured. We experimentally show the usefulness of this method in the following three cases: where a silica-based SMF is butt-coupled to 1) a silica-based GI-MMF with 50-μm core diameter; 2) a perfluorinated GI polymer optical fiber (PFGI-POF) with 62.5-μm core diameter; and 3) a PFGI-POF with 120-μm core diameter. Depending on the relative core position, not only the Stokes power but also the Brillouin frequency shift changed, which probably originates from the excitation of higher order modes.**

***Index Terms*—Brillouin frequency shift (BFS), Brillouin scattering, butt coupling, core alignment, graded-index multimode optical fiber (GI-MMF), nonlinear optics, polymer optical fiber.**

I. Introduction

FIBER-OPTIC sensors have a number of advantages compared to other sensor elements, such as flexibility, light weight, tolerance of electromagnetic interference, etc., and have been widely studied as a promising technology for achieving smart materials and structures [1]–[7]. Recently, graded-index multimode optical fibers (GI-MMFs) [8]–[10] including graded-index polymer optical fibers (GI-POFs) [11]–[16] have attracted considerable attention as sensing heads, because their fracture toughness and flexibility can make the systems much easier to handle in field applications. It is generally difficult to implement all the optical parts of the sensing systems using GI-MMFs only, because most of the optical devices, such as lasers, isolators, couplers, circulators, and amplifiers, are composed of single-mode optical fibers (SMFs). Therefore, it is extremely important to optically couple an SMF and a GI-MMF with high efficiency.

If connectors (FC, SC, LC, etc.) are attached to both ends of the fibers to be coupled, we can easily align the relative core position by employing a proper adapter. However, when such connectors are not available, we must align the relative core position to achieve highly efficient butt coupling with one of the fibers fixed on a multiaxis positioning stage. In general, the alignment is optimized by monitoring and maximizing the power of transmitted light at the output end of the GI-MMF, but in some cases it is difficult to measure the power. For example: 1) when the GI-MMF is embedded in structures as a sensing head; 2) when the output end of the GI-MMF is located quite far away; and 3) when the light propagation loss in the GI-MMF is extremely high. In these cases, the butt-coupling efficiency needs to be optimized only from the incident side. In commercially available fiber splicers, charge-coupled device cameras are often used for this purpose, but they are expensive and not easy to handle.

Another approach is to make use of reflected light, with which more accurate core alignment is potentially feasible, because the light beams propagating in the GI-MMF are concentrated in the core center. However, the light reflected from the GI-MMF, mostly due to Rayleigh scattering, is mixed with unstable Fresnel-reflected light generated at the coupling boundaries. Therefore, the power of the reflected light becomes so unstable that it is difficult to simply use it for accurate core alignment. One way to separate the Fresnel-reflected light is to utilize the light reflected from the GI-MMF due to nonlinear scattering with frequency shift, such as Brillouin scattering and Raman scattering. Brillouin scattering seems to be the more suitable of the two, because it is known to have lower frequency shift, narrower bandwidth, and lower threshold, i.e., higher Stokes power than backward Raman scattering [17].

In this paper, we experimentally demonstrate that the butt-coupling efficiency between an SMF and GI-MMFs can be optimized by monitoring and maximizing the power of the Brillouin-scattered light. Three different GI-MMFs are employed: 1) a silica-based GI-MMF with 50-μm core diameter; 2) a perfluorinated GI-POF (PFGI-POF) with 62.5-μm core diameter; and 3) a PFGI-POF with 120-μm core diameter, and these experimental results well explain the usefulness of this method. Besides, we show that not only the Stokes power but also the Brillouin frequency shift (BFS) changes depending on the relative core position. This is probably because of the excitation of higher order modes with different BFS.

Manuscript received April 03, 2011; revised June 08, 2011; accepted July 05, 2011. The work of Y. Mizuno was supported by the Research Fellowships for Young Scientists from the Japan Society for the Promotion of Science.

The authors are with Precision and Intelligence Laboratory, Tokyo Institute of Technology, Kanagawa 226-8503, Japan (e-mail: ymizuno@sonic.pi.titech.ac.jp, knakamur@sonic.pi.titech.ac.jp).

Color versions of one or more of the figures in this paper are available online at http://ieeexplore.ieee.org.

Digital Object Identifier 10.1109/JLT.2011.2161754

TABLE I
PHYSICAL PROPERTIES OF THE SILICA SMF, SILICA GI-MMF, AND PFGI-POFs. d, CORE DIAMETER; n_{eff}, EFFECTIVE CORE REFRACTIVE INDEX; NA, NUMERICAL APERTURE; α, PROPAGATION LOSS; L, FIBER LENGTH

Fiber	d (μm)	n_{eff}	NA	α (dB/km)	L (m)
Silica SMF	8	~1.47	0.13	~0.5	1.6
Silica GI-MMF	50	~1.46	0.2	~1.0	100
PFGI-POF (A)	62.5	~1.35	0.185	~150	5
PFGI-POF (B)	120	~1.35	0.185	~150	100

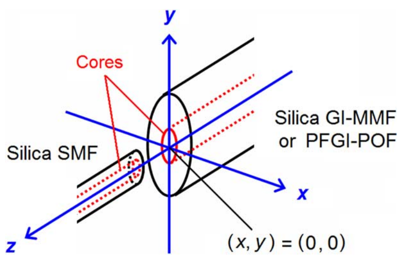

Fig. 1. Schematic of core alignment, where an SMF is butt-coupled to a GI-MMF. The z axis is defined as the fiber axis direction, and the xy plane is defined as the plane perpendicular to the z-axis. Both x and y are defined to be zero when the core alignment is optimal.

II. EXPERIMENTAL SETUP

We used a standard silica-based SMF and three kinds of GI-MMFs: one silica-based GI-MMF and two PFGI-POFs. Their physical properties are summarized in Table I.

The position of the SMF was fixed, and the GI-MMFs were mounted on a three axis positioning stage. Here, we define each axis as shown in Fig. 1. The alignment procedure was as follows. First, the relative angle of the fibers to be coupled was roughly adjusted. Next, index-matching oil ($n = 1.46$) was placed on one of the fiber ends to fill the air gap and suppress the Fresnel reflection [18]. Then, the z axis was adjusted so that the distance between the two fiber ends became nearly zero. In this step, angular misalignment was automatically compensated. Finally, x- and y-axes were adjusted using the Brillouin-based method.

The whole experimental setup for detecting the Brillouin signal is depicted in Fig. 2. The output light of a distributed-feedback laser diode (DFB-LD) at 1552 nm was divided into pump light and reference light. The pump light was amplified with a moderate-power erbium-doped fiber amplifier (EDFA) and injected into GI-MMFs via butt coupling. A polarization controller (PC) was used to suppress polarization-dependent fluctuations of the signal. The Brillouin-scattered Stokes light was heterodyned with the polarization-optimized reference light, and the optical beat signal was converted to an electrical signal with a photodetector (PD). The signal was preamplified by 23 dB, and monitored with an electrical spectrum analyzer (ESA). Here, a 9-GHz frequency shifter (FS) was used to monitor the Brillouin signal of a silica GI-MMF (typical BFS ~11 GHz), because the bandwidths of the preamplifier and the ESA were 0.9–4.5 GHz and 9 kHz–8.1 GHz, respectively. When the Brillouin signal is sufficiently large, the EDFA, PCs, and preamplifier need not be employed.

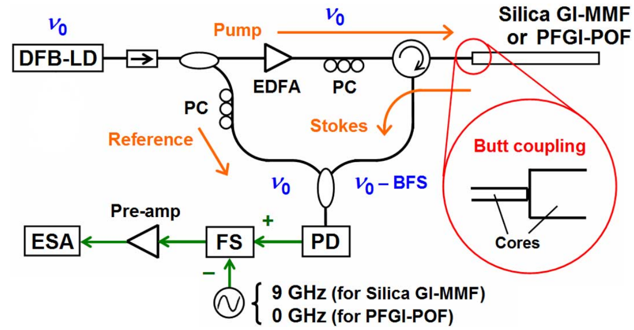

Fig. 2. Experimental setup of the core alignment system. DFB-LD, distributed-feedback laser diode; EDFA, erbium-doped fiber amplifier; ESA, electrical spectrum analyzer; FS, frequency shifter; PC, polarization controller; PD, photodetector.

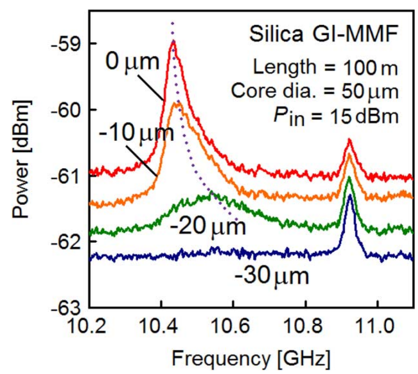

Fig. 3. BGSs of the silica GI-MMF when x (relative distance from the optimal position) was 0, -10, -20, and -30 μm with y fixed at 0 μm.

III. RESULTS AND DISCUSSIONS

Experimental results and discussions are presented in this section, which are classified according to the types of the GI fibers used (See Table I).

A. Silica GI-MMF

Fig. 3 shows the dependence of the Brillouin gain spectrum (BGS) on x with y fixed at 0 μm, i.e., on the relative distance from the optimal core position. The optical power at the end of the SMF P_{in} was 15 dBm. Two peaks were observed; one around 10.5 GHz corresponds to the Brillouin Stokes signal of the silica GI-MMF, and the other at 10.92 GHz to that of the SMF. As the absolute value of x, $|x|$, increased, the Stokes peak power of the GI-MMF drastically decreased. The peak power of the SMF also slightly decreased due to the polarization-dependent fluctuations, which are so unstable that it is difficult to use this effect to align the core.

Fig. 4 shows the x-dependence of the Stokes peak power of the GI-MMF. The x-dependence of the transmission power measured with an optical power meter is also provided, which is normalized so that its peak power is 0 dB. The Stokes power was maximum when $x = 0$ μm, and monotonically decreased as $|x|$ increased, just in the same way as the transmission power. Outside the core region of the GI-MMF, i.e., when $|x| > 25$ μm, the Brillouin signal was completely buried by the noise floor. This behavior was well fitted by a Gaussian curve. Thus, it was shown that efficient core alignment is feasible by monitoring

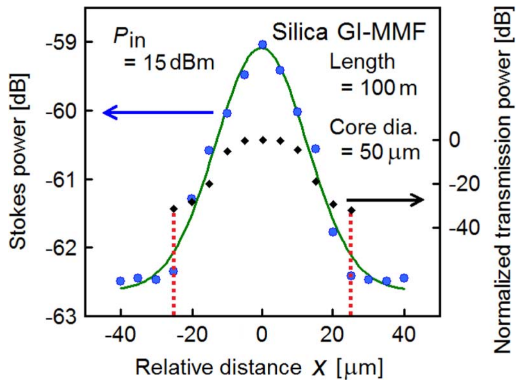

Fig. 4. Stokes power and normalized transmission power of the silica GI-MMF as functions of relative distance x. The solid line shows a Gaussian fit, and the dotted vertical lines indicate the core boundaries.

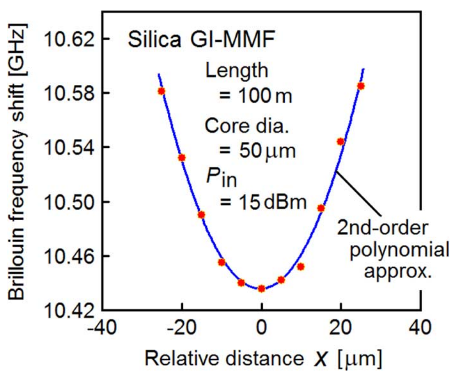

Fig. 5. BFS of the silica GI-MMF versus relative distance x. The solid line shows a second-order polynomial fit.

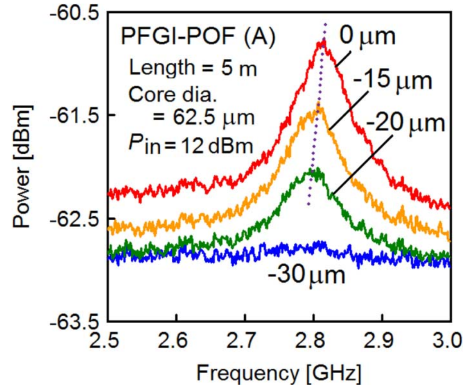

Fig. 6. BGS of the PFGI-POF (A) when x was 0, -15, -20, and -30 μm.

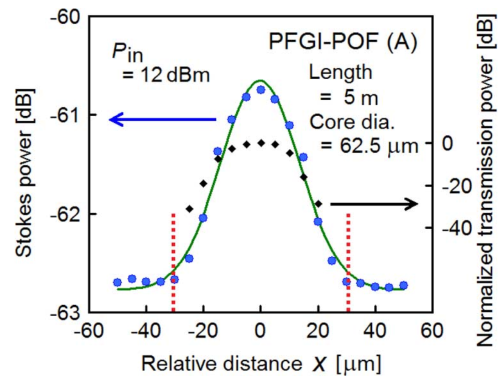

Fig. 7. Stokes power and normalized transmission power of the PFGI-POF (A) as functions of x. The solid line shows a Gaussian fit, and the dotted vertical lines indicate the core boundaries.

and maximizing the Brillouin Stokes power of the GI-MMF. Even when the BGS of the GI-MMF happens to overlap that of the SMF, this method is available unless the BGS of the GI-MMF is extremely small.

In Fig. 3, we notice that not only the Stokes power but also the frequency shift, called BFS, of the GI-MMF is also dependent on x. Fig. 5 shows the BFS as a function of x, where the BFS changed in proportion to the square of $|x|$. This indicates that the core alignment can be performed not only by maximizing the Stokes power but also by minimizing the BFS. This effect seems to originate from the excitation of many higher order modes with different Brillouin frequencies, which is also the reason for the broadening of the Brillouin bandwidth with the increasing x, seen in Fig. 3.

B. PFGI-POF (A)

The x-dependence of the BGS in the PFGI-POF with 62.5-μm core diameter is shown in Fig. 6. The optical input power $P_{\rm in}$ was fixed at 12 dBm. Since the BFS of PFGI-POFs is approximately four times lower than that of silica-based fibers [19], only one Brillouin peak of the PFGI-POF was observed in the range of 2.5–3.0 GHz. The x-dependences of the Stokes power and the normalized transmission power shown in Fig. 7 were similar to those of the silica GI-MMF, which confirms that this alignment method can be applied also to the coupling of the fibers composed of different materials.

Compared to the case of silica GI-MMF, the x-dependence of the BFS was extremely small, and the sign of its coefficient was opposite, as seen in Fig. 6. In this case, we cannot align the core accurately by maximizing the BFS.

C. PFGI-POF (B)

The x-dependences of the BGS in the PFGI-POF with 120-μm core diameter when $x \geq 0$ and $x \leq 0$ are shown in Figs. 8 and 9, respectively. The input power was fixed at 15 dBm. In Fig. 8, the peak power and the BFS behaved in the same way as those in Fig. 6. In contrast, in Fig. 9, the peak power hardly changed while x was in the range of -40 to -30 μm. We confirmed using a fiber microscope that this irregular behavior was due to the relatively rough surface of the PFGI-POF end. In general, it is difficult to make a highly smooth surface by polishing the end of large-core PFGI-POFs, because they are much softer and more easily damaged than silica fibers.

The dependence of the Stokes power on x is shown in Fig. 10. As shown in the figure, even when there are some irregular points originating from the rough surface, they have little influence on core alignment itself. Instead, we can roughly estimate the smoothness of the fiber end surface by detecting such irregular points.

IV. Conclusion

We demonstrated that highly efficient butt coupling between an SMF and GI-MMFs is easily achievable by monitoring and

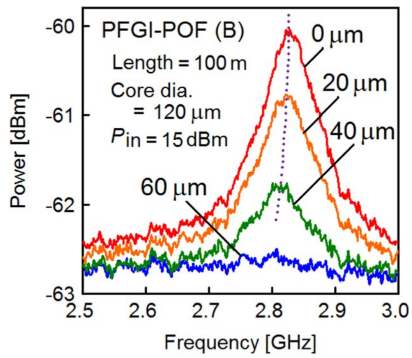

Fig. 8. BGS of the PFGI-POF (B) when x was 0, 20, 40, and 60 μm.

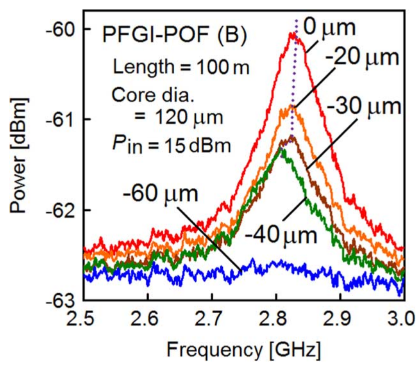

Fig. 9. BGS of the PFGI-POF (B) when x was 0, -20, -30, -40, and -60 μm.

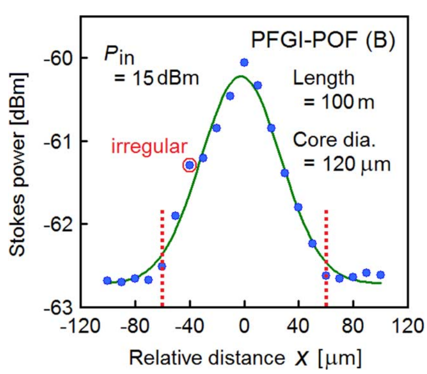

Fig. 10. Stokes power of the PFGI-POF (B) as a function of x. The solid line shows a Gaussian fit without using the irregular data at $x = -40$ μm, and the dotted lines indicate the core boundaries.

maximizing the power of the Brillouin-scattered light. The usefulness of this method was confirmed by the experimental results with three different GI-MMFs. Furthermore, we found that the BFS also depends on the relative core position due to the excitation of many higher order modes. We believe this Brillouin-based core alignment method will greatly help GI-MMFs including GI-POFs to be utilized as sensing heads in fiber-optic sensing systems with ease of handling, fracture toughness, and high flexibility.

Acknowledgment

The authors are grateful to Sekisui Chemical Co., Ltd., for providing the PFGI-POF samples. They are also thankful to Prof. T. Ishigure at Keio University for his helpful discussions and comments. In addition, they would like to thank an anonymous reviewer of an earlier version of this paper for his/her constructive and insightful comments and suggestions.

References

[1] J. Dakin and B. Culshaw, *Optical Fiber Sensors: Principles and Components*. Norwood, MA: Artech House, 1988.

[2] D. A. Jackson, "Monomode optical fiber interferometers for precision measurement," *J. Phys. E.: Sci. Instrum.*, vol. 18, pp. 981–1001, 1985.

[3] K. Hotate, "Fiber sensor technology today," *Jpn. J. Appl. Phys.*, vol. 45, pp. 6616–6625, 2006.

[4] T. Horiguchi and M. Tateda, "BOTDA—Nondestructive measurement of single-mode optical fiber attenuation characteristics using Brillouin interaction: Theory," *J. Lightw. Technol.*, vol. 7, no. 8, pp. 1170–1176, Aug. 1989.

[5] D. Garus, K. Krebber, F. Schliep, and T. Gogolla, "Distributed sensing technique based on Brillouin optical-fiber frequency-domain analysis," *Opt. Lett.*, vol. 21, pp. 1402–1404, 1996.

[6] K. Hotate and T. Hasegawa, "Measurement of Brillouin gain spectrum distribution along an optical fiber using a correlation-based technique—Proposal, experiment and simulation," *IEICE Trans. Electron.*, vol. E83-C, pp. 405–412, 2000.

[7] Y. Mizuno, W. Zou, Z. He, and K. Hotate, "Proposal of Brillouin optical correlation-domain reflectometry (BOCDR)," *Opt. Exp.*, vol. 16, pp. 12148–12153, 2008.

[8] P. Lenke and N. Nöther, "Stimulated Brillouin scattering in graded index multimode optical fiber by excitation of the fundamental mode only," in *Proc. Int. Soc. Opt. Eng.*, 2007, vol. 6582, p. 658213.

[9] D. Donlagic and B. Culshaw, "Propagation of the fundamental mode in curved graded index multimode fiber and its application in sensor systems," *J. Lightw. Technol.*, vol. 18, no. 3, pp. 334–342, Mar. 2000.

[10] W. Zhao and R. O. Claus, "Optical fiber grating sensors in multimode fibers," *Smart Mater. Struct.*, vol. 9, pp. 212–214, 2000.

[11] K. Peters, "Polymer optical fiber sensors—A review," *Smart Mater. Struct.*, vol. 20, p. 013002, 2010.

[12] Y. Mizuno and K. Nakamura, "Potential of Brillouin scattering in polymer optical fiber for strain-insensitive high-accuracy temperature sensing," *Opt. Lett.*, vol. 35, pp. 3985–3987, 2010.

[13] S. Liehr, P. Lenke, M. Wendt, K. Krebber, M. Seeger, E. Thiele, H. Metschies, B. Gebreselassie, and J. C. Munich, "Polymer optical fiber sensors for distributed strain measurement and application in structural health monitoring," *IEEE Sens. J.*, vol. 9, no. 11, pp. 1330–1338, Nov. 2009.

[14] I. R. Husdi, K. Nakamura, and S. Ueha, "Sensing characteristics of plastic optical fibres measured by optical time-domain reflectometry," *Meas. Sci. Technol.*, vol. 15, pp. 1553–1559, 2004.

[15] S. Kiesel, K. Peters, T. Hassan, and M. Kowalsky, "Calibration of a single-mode polymer optical fiber large-strain sensor," *Meas. Sci. Technol.*, vol. 20, p. 034016, 2009.

[16] S. T. Kreger, A. K. Sang, D. K. Gifford, and M. E. Froggatt, "Distributed strain and temperature sensing in plastic optical fiber using Rayleigh scatter," in *Proc. Int. Soc. Opt. Eng.*, 2009, vol. 7316, p. 73160A.

[17] G. P. Agrawal, *Nonlinear Fiber Optics*. San Diego, CA: Academic, 1995.

[18] Y. Mizuno, W. Zou, and K. Nakamura, "Fresnel reflection spectra at multimode optical fiber ends with heterodyne detection," *Appl. Phys. Exp.*, vol. 4, p. 012501, 2011.

[19] Y. Mizuno and K. Nakamura, "Experimental study of Brillouin scattering in perfluorinated polymer optical fiber at telecommunication wavelength," *Appl. Phys. Lett.*, vol. 97, p. 021103, 2010.

Yosuke Mizuno was born in Hyogo, Japan, on October 13, 1982. He received the B.E., M.E., and Dr. Eng. degrees in electronic engineering from the University of Tokyo, Tokyo, Japan, in 2005, 2007, and 2010, respectively.

In 2004, he was involved in optical information processing at the University of Tokyo. From 2005 to 2007, he was involved in spin electronics, and studied spin hot-carrier transistors for his master degree. From 2007 to 2010, he was involved in Brillouin optical correlation-domain reflectometry for his Dr. Eng. degree at the University of Tokyo. In 2010, he became a Postdoctoral Research Fellow of Tokyo Institute of Technology, Kanagawa, Japan. His research interests include fiber-optic sensors, polymer optics, and ultrasonics.

Dr. Mizuno is a member of the Japanese Society of Applied Physics, and the Institute of Electronics, Information, and Communication Engineers of Japan.

From 2007 to 2010, he was a Research Fellow, DC1, of the Japan Society for the Promotion of Science (JSPS). He is currently a Research Fellow, PD, of JSPS.

Kentaro Nakamura (M'00) was born in Tokyo, Japan, on July 3, 1963. He received the B.E., M.E., and Dr. Eng. degrees from the Tokyo Institute of Technology, Kanagawa, Japan, in 1987, 1989, and 1992, respectively.

Since 2010, he has been a Professor at the Precision and Intelligence Laboratory, Tokyo Institute of Technology. His research interests include the application of ultrasonics and the measurement of vibration and sound using optical methods as well as fiber-optic sensors.

Dr. Nakamura received the Awaya Kiyoshi Award from the Acoustical Society of Japan (ASJ) in 1996. He received the best paper awards from the Institute of Electronics, Information and Communication Engineers in 1998 and from Ultrasonic Electronics in 2007, respectively. He received the *Japanese Journal of Applied Physics* Editorial Contribution Award from the Japan Society of Applied Physics in 2007. Since 2009, he has been the Vice President of ASJ.